

High-frequency electromagnetic waves destabilized by runaway electrons in a near-critical electric field

A. Kómár¹, T. Fülöp², G.I. Pokol¹

¹ Department of Nuclear Techniques, Budapest University of Technology and Economics, Association EURATOM, H-1111 Budapest, Hungary

² Department of Applied Physics, Chalmers University of Technology and Euratom-VR Association, Göteborg, Sweden

Introduction Runaway electron distributions with strong velocity space anisotropy may destabilize high-frequency electromagnetic waves through a resonant interaction. Such an interaction was studied previously in a case when the electric field is much higher than the critical field for runaway acceleration and secondary runaway generation dominates [1-3]. However, it was recently pointed out that even in large tokamak disruptions the electric field on axis is only slightly higher than the critical field [4]. Therefore, in this work we investigate the lowest relevant limit, the near-critical case. This provides us with insight to the electric field dependence of the results, and opens the way toward calculations with arbitrary runaway distributions.

Distribution function In the near-critical case the electric field is low and primary generation is the dominant method of runaway generation. Thus, in the present work, a distribution function relevant for this case will be used [5], with $\alpha = E/E_c \gtrsim 1$, where E is the electric field, E_c is the critical field. The distribution, obtained by matching solutions of the Fokker-Planck equation in five different regions of momentum space is

$$f_r(p_{\parallel}, p_{\perp}) = \frac{A}{p_{\parallel}^{(C_s-2)/(\alpha-1)}} \exp\left(-\frac{(\alpha+1)p_{\perp}^2}{2(1+Z)p_{\parallel}}\right) {}_1F_1\left(1 - \frac{C_s}{\alpha+1}, 1; \frac{(\alpha+1)p_{\perp}^2}{2(1+Z)p_{\parallel}}\right), \quad (1)$$

where $C_s = \alpha - \frac{(1+Z)}{4}(\alpha-2)\sqrt{\frac{\alpha}{\alpha-1}}$, Z is the effective ion charge, ${}_1F_1$ is the confluent hypergeometric (Kummer) function and A is a normalization constant. The distribution is positive on all of the momentum space only if the first argument of ${}_1F_1$ is positive: $C_s < \alpha+1$. Furthermore, the condition $f_r \rightarrow 0$ for $p_{\parallel} \rightarrow \infty$ requires that $C_s > 2$. These two conditions define a region in the $\alpha - Z$ space where the distribution is valid (see Fig. 1a). On Fig. 1b, the normalized distribution is plotted for $\alpha = 1.3$, $Z = 1$, where \parallel/\perp indices denote parallel/perpendicular directions to the static magnetic field. By comparing this distribution to the one relevant in high electric fields [1-3] (Fig. 1c), it can be seen that the anisotropy is much weaker in the near-critical distribution. Also, because of the primary generation of runaways, the tail of the steady-state distribution (1) is not exponentially decaying but slower.

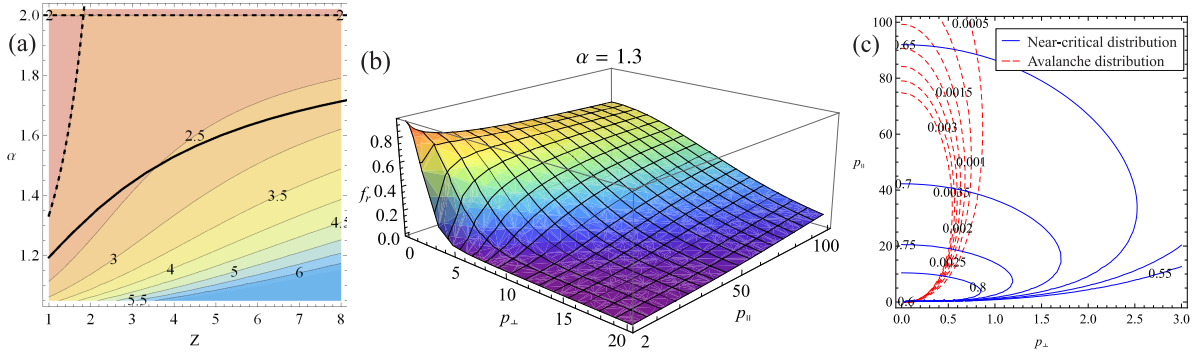


Figure 1: (a) C_s plotted with respect to α and Z , f_r is valid in between the black lines. (b,c) Normalized runaway distribution as function of the momentum normalized to $m_e c$ in the near-critical case, (b) for $\alpha = E/E_c = 1.3$ and $Z = 1$ effective ion charge, (c) compared to the distribution valid in high electric fields for $\alpha = 800$, $Z = 1$ and $\ln \Lambda = 18$.

Wave dispersion When deriving the dispersion of the high-frequency electromagnetic waves we used the cold plasma approximation, which has proved to be valid for temperatures as high as 20 keV. With the electromagnetic approximation, $\epsilon_{33}^{e+i} \gg k_{\parallel} k_{\perp} c^2 / \omega^2$, the dispersion yields $(\epsilon_{11} - k_{\parallel}^2 c^2 / \omega^2)(\epsilon_{22} - k^2 c^2 / \omega^2) + \epsilon_{12}^2 = 0$, where ω is the wave frequency, k is the wave number and ϵ is the dielectric tensor of the plasma, consisting of the susceptibilities of the different plasma species: $\epsilon = \mathbf{1} + \chi^i + \chi^e + \chi^r$, the indices i , e and r denoting the ion, thermal electron and runaway population.

Two different approximations are used, one where $\omega \gg \omega_{ce} \sqrt{m_e/m_i}$, for which the dielectric tensor is $\epsilon_{11}^{e+i} = 1 - \omega_{pe}^2/(\omega^2 - \omega_{ce}^2)$, $\epsilon_{22}^{e+i} = 1 - \omega_{pe}^2/(\omega^2 - \omega_{ce}^2)$, $\epsilon_{12}^{e+i} = -i\omega_{pe}^2 \omega_{ce}/[\omega(\omega^2 - \omega_{ce}^2)]$, where ω_{pe} is the electron plasma- and ω_{ce} is the electron cyclotron frequency. This dispersion defines three different electromagnetic waves, of which we used the lowest frequency branch and named it ‘electron-whistler wave’ because for certain limits it overlaps with the whistler wave defined in Ref. [6]. The other approximation is the magnetosonic-whistler wave of Refs. [1-3] with the difference of keeping the ones from the dyadic unit in the dielectric tensor elements (valid for $\omega_{ci} \ll \omega \ll \omega_{ce}$): $\epsilon_{11}^{e+i} = 1 - \omega_{pi}^2/\omega^2 + \omega_{pe}^2/\omega_{ce}^2$, $\epsilon_{22}^{e+i} = 1 - \omega_{pi}^2/\omega^2 + \omega_{pi}^2/\omega_{ci} \omega_{ce}$, $\epsilon_{12}^{e+i} = i\omega_{pi}^2/\omega_{ci} \omega$, where ω_{pi} is the ion plasma- and ω_{ci} is the ion cyclotron frequency. The two different approximations are plotted on Fig. 2, where $\cos \theta = k_{\parallel}/k$. They overlap in the region around $k \sim 5 \text{ cm}^{-1}$, otherwise the magnetosonic-

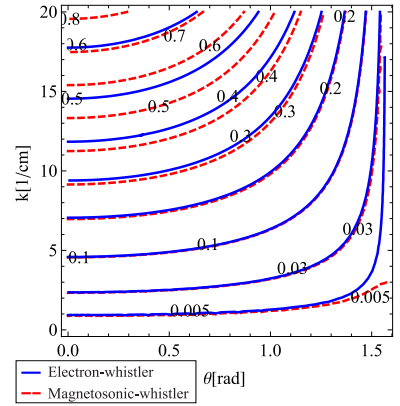


Figure 2: Comparison of the electron- and magnetosonic-whistler (ω/ω_{ce}) for density $n_e = n_i = 5 \cdot 10^{19} \text{ m}^{-3}$, magnetic field $B = 2 \text{ T}$.

whistler wave is valid for lower wave numbers while the electron-whistler is valid for high wave numbers.

Growth rate In the presence of runaway electrons, the linear growth rate of the waves can be calculated by perturbing the dispersion with the runaway susceptibility. This results in an additional $\delta\omega$ term in the wave frequency, the imaginary part of which is the linear growth rate γ_i . The growth rate can thus be calculated from the unperturbed dispersion and the runaway susceptibility. The resonance condition giving the momentum of the runaway electrons resonant with the wave is $p_{\parallel}k_{\parallel}c + n\omega_{ce} - \omega\gamma = 0$, where $\gamma = \sqrt{1 + p^2}$ is the relativistic factor and n is the order of resonance. In previous studies, the relativistic factor was approximated as $\gamma \approx |p_{\parallel}|$, and this led to the so-called ultrarelativistic resonance condition. However, this approximation does not hold if the accelerating electric field is lower. Thus, in this work the general form of the resonance condition was used, obtained by substituting the full expression for γ into the resonance condition.

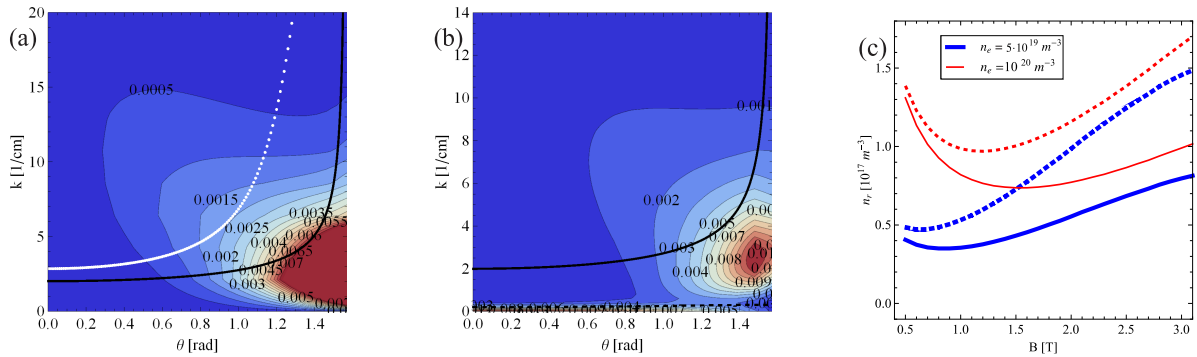


Figure 3: (a,b) Growth rates (γ_i/ω_{ce}) of (a) the electron-whistler, (b) the magnetosonic-whistler wave for resonances $n = 0, -1$, runaway density $n_r = 3 \cdot 10^{17} \text{ m}^{-3}$ and for $n_e = n_i = 5 \cdot 10^{19} \text{ m}^{-3}$, $B = 2 \text{ T}$. The black line is $\omega = \omega_{ce}/45$, the white dots correspond to the runaway energy of 2.6 MeV. (c) Stability diagram for the electron-whistler wave for runaway beam radius $L_r = 0.1 \text{ m}$ (dashed) and 0.2 m (solid).

The growth rate of the electron- and magnetosonic-whistler waves are presented on Fig. 3ab. They are positive, with a maximum in the magnetosonic-whistler region, around $k_m \sim 2 \text{ cm}^{-1}$ and $\theta_m \sim \pi/2$ for the parameters given in the figure caption. Nevertheless, the wave with these parameters is the most unstable wave only if the runaways reach the corresponding resonant energy of 10 MeV. Reaching this energy is unlikely in a near-critical field, so the parameters of the most unstable wave depend on the maximum runaway energy. The $k(\theta)$ curve corresponding to the energy of 2.6 MeV is plotted on Fig. 3a, and the growth rate is only valid for wave numbers higher than this line, i.e. in the region which corresponds to lower runaway energies. From the figure we can deduce that

the most unstable wave will be the one destabilized by the maximum energy runaways, an electron-whistler wave of oblique propagation.

The dependence of the parameters of the most unstable wave on the maximum runaway energy was investigated, and we came to the conclusion, that for higher resonant energy the wave number of the most unstable wave decreases while its propagation angle increases, resulting in a decreasing wave frequency, see Fig. 4ab.

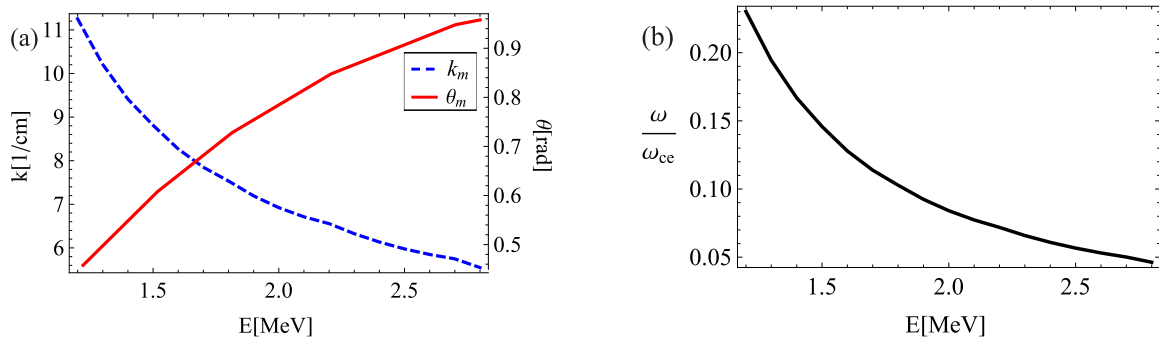


Figure 4: *Parameters of the most unstable wave as a function of the resonant energy (a) wave number and propagation angle, (b) wave frequency.*

The growth rate of the most unstable electron-whistler wave for 2.6 MeV maximum energy was compared to the collisional and convective damping rates for $T_e = 20$ eV post-disruption electron temperature, and a stability threshold was determined. If the runaway density is higher than the critical values plotted on Fig. 3c, the wave is destabilized. The density threshold is higher for a narrower runaway beam, as well as for a higher magnetic field, in the region of validity of our approximations, between 1 – 3 T.

Conclusions Our results show that the interaction between runaway electrons and electromagnetic waves is similar in the near-critical and high electric field case in the sense that neither the runaway distributions nor the growth rates differ qualitatively. The generalizations presented here are necessary in order to expand the validity of the calculations for lower electric fields. They are also essential for the numerical handling of the problem, needed when proceeding to the evaluation of arbitrary distribution functions.

Acknowledgments This work was funded by the European Communities under Association Contract between EURATOM, HAS and *Vetenskapsrådet*. One of the authors acknowledges the financial support from the FUSENET Association.

- [1] T. Fülöp et al., *Phys. Plasmas* **13**, 062506 (2006).
- [2] G. Pokol et al., *Plasma Phys. Control. Fusion* **50**, 045003 (2008).
- [3] T. Fülöp et al., *Phys. Plasmas* **16**, 022502 (2009).
- [4] J. Riemann et al., *Phys. Plasmas* **19**, 012507 (2012).
- [5] P. Sandquist et al., *Phys. Plasmas*, **13** 072108 (2006).
- [6] T. H. Stix, *Waves in plasmas*, American Institute of Physics, New York (1992).